



# Light Induced Changes in Pigment and Lipid Profiles of Bryopsidales Algae

Chiara E. Giossi<sup>1†</sup>, Sónia Cruz<sup>1</sup>, Felisa Rey<sup>2,3</sup>, Rúben Marques<sup>1</sup>, Tânia Melo<sup>2,3</sup>, Maria do Rosário Domingues<sup>2,3</sup> and Paulo Cartaxana<sup>1\*</sup>

<sup>1</sup> Centre for Environmental and Marine Studies, Department of Biology, University of Aveiro, Aveiro, Portugal, <sup>2</sup> Centre for Environmental and Marine Studies, Department of Chemistry, University of Aveiro, Aveiro, Portugal, <sup>3</sup> Mass Spectrometry Centre, LAQV-REQUIMTE, Department of Chemistry, University of Aveiro, Aveiro, Portugal

## OPEN ACCESS

### Edited by:

Andrew Stanley Mount,  
Clemson University, United States

### Reviewed by:

Alexei E. Solovchenko,  
Lomonosov Moscow State University,  
Russia

Olga Dymova,  
Institute of Biology, Komi Scientific  
Center, Russian Academy of Sciences  
(RAS), Russia

### \*Correspondence:

Paulo Cartaxana  
pcartaxana@ua.pt

### † Present address:

Chiara E. Giossi,  
Plant Ecophysiology, Department of  
Biology, University of Konstanz,  
Konstanz, Germany

### Specialty section:

This article was submitted to  
Marine Molecular Biology  
and Ecology,  
a section of the journal  
Frontiers in Marine Science

Received: 21 July 2021

Accepted: 16 August 2021

Published: 06 September 2021

### Citation:

Giossi CE, Cruz S, Rey F,  
Marques R, Melo T, Domingues MR  
and Cartaxana P (2021) Light Induced  
Changes in Pigment and Lipid Profiles  
of Bryopsidales Algae.  
Front. Mar. Sci. 8:745083.  
doi: 10.3389/fmars.2021.745083

Bryopsidales (Chlorophyta) are cultured and consumed in several regions of the planet and are known for their high nutritional value and bioprospection potential, due to a high content of relevant polar lipids and polysaccharides. Among other characteristic features, these marine algae are known for possessing unique photosynthetic pigment-protein complexes and for the absence (in nearly all species investigated) of a functional xanthophyll cycle, a ubiquitous photoprotection mechanism present in most algae and plants. With the aim of characterizing the photophysiology of this atypical group of algae, we investigated the changes in pigment content and polar lipidome of two Bryopsidales species (*Codium tomentosum* and *Bryopsis plumosa*) exposed for 7 days to low or high irradiance (20 vs. 1,000  $\mu\text{mol photons m}^{-2} \text{s}^{-1}$ ). Our results show that high light has a strong effect on the pigment composition, triggering the time-dependent accumulation of all-*trans*-neoxanthin (*t*-Neo) and violaxanthin (Viola). High light-acclimated macroalgae also displayed a shift in the characteristic polar lipidome, including a trend of accumulation of lyso-glycolipids, and highly unsaturated phospholipids and betaine lipids. We hypothesize that the observed shifts on the lipid composition could promote the interaction between *t*-Neo and Viola with the siphonaxanthin-chlorophyll-protein complexes (SCP) of photosystem II (PSII) within the thylakoid membranes of the chloroplasts. Light induced changes in pigment and lipid composition could contribute to the fitness of Bryopsidales algae by reducing damages to the photosynthetic apparatus under increased irradiance.

**Keywords:** *Bryopsis plumosa*, *Codium tomentosum*, green algae, light acclimation, photophysiology, lipidomics, all-*trans*-neoxanthin, xanthophylls

## INTRODUCTION

Bryopsidales is a monophyletic order of siphonous green algae with high ecological relevance in both tropical and temperate marine coastal ecosystems (Cremen et al., 2019). Recently, these organisms have received increasing attention due to their remarkable content of valuable polar lipids and polysaccharides with potential pharmaceutical and nutraceutical applications (e.g., Maeda et al., 2012; Arata et al., 2015; Santos et al., 2015; Fleurence and Levine, 2016). Furthermore,

some species of the genera *Codium* and *Caulerpa* are amongst the most popular edible macroalgae and listed as delicacies in gourmet cuisine (Paul et al., 2014; Pérez-Lloréns et al., 2018).

Despite their relevance on both ecological and economical levels, the photophysiology of Bryopsidales is poorly understood. The photosynthetic antennae of these macroalgae are characterized by the unique association of the xanthophylls siphonaxanthin and its esterified form siphonaxanthin-dodecenoate (also referred to as siphonein) at the level of the photosynthetic antennae, together with chlorophylls *a* and *b* (Kageyama et al., 1977; Yokohama et al., 1977; Nakayama and Okada, 1990). These siphonaxanthin-type light harvesting complexes are responsible for an increased absorption in the green and blue-green light regions, predominant in deep waters or shaded subtidal marine habitats (Anderson, 1983; Wang et al., 2013). In recent years, it has also been reported that several species of Bryopsidales lack a functional xanthophyll cycle (Cruz et al., 2015; Christa et al., 2017; Giovagnetti et al., 2018), a common photoprotection mechanism present in most algae and higher plants (Latowski et al., 2011; Goss and Lepetit, 2015). The most common xanthophyll cycle comprises the sequential de-epoxidation of the pigments violaxanthin (Viola) to antheraxanthin and zeaxanthin under high light, allowing excess energy dissipation as heat. On the other hand, the accumulation of the xanthophylls all-*trans*-neoxanthin (*t*-Neo) and Viola, putatively involved in photoprotection, have been reported in Bryopsidales macroalgae under high light (Uragami et al., 2014; Cartaxana et al., 2018). However, the mechanisms of photoprotection necessary for these algae to cope with increased irradiance, particularly relevant in their natural habitats during low tides or summer, remain largely unexplored.

In this work, we investigated photophysiological changes in two different Bryopsidales species, *Codium tomentosum* (Stackhouse, 1797) and *Bryopsis plumosa* (Agardh, 1823), with the aim of identifying key players involved in photoprotection and/or in enhancing the photosynthetic performance under increased irradiance, by (i) characterizing the time-dependent changes in the pigment composition in response to high light and (ii) analyzing the changes in the polar lipidome in high light acclimated algae, focusing on lipid classes with known relevance for the structure and functionality of chloroplast membranes and molecules possibly involved in photoprotection. Our results show that high irradiance triggers time-dependent accumulation of the putative photoprotective xanthophylls *t*-Neo and Viola and a shift in the polar lipidome that could correspond to a rearrangement of chloroplast membranes, possibly allowing a better photosynthetic performance under high light. Potential interactions between the theorized photoprotective model involving *t*-Neo (Uragami et al., 2014) and the observed alterations in the polar lipidome are discussed.

## MATERIALS AND METHODS

### Algae Collection and Cultivation

Wild specimens of *C. tomentosum* were collected from the rocky shores of Aguda beach, Portugal (41° 04' 66.22" N, 8° 65' 32.72"

W) in May 2019 during low tide. *B. plumosa* was acquired from Kobe University Macroalgal Culture Collection (KU-0990, KU-MACC, Japan). Prior to treatments, macroalgae were maintained in a thermostatically controlled room (17°C), with aeration and long day photoperiod (16/8 h, light/dark) and an irradiance of 130  $\mu\text{mol photons m}^{-2} \text{s}^{-1}$  (FLUORA T8, L58 W/77, OSRAM). Medium *f*/2 supplemented with 1  $\text{mg L}^{-1}$   $\text{GeO}_2$  was prepared according to Andersen (2005). For experiments, algae were pre-cultured under Low Light (LL, 20  $\mu\text{mol photons m}^{-2} \text{s}^{-1}$ ) for 1 week. Subsequently, they were exposed for seven days to High Light (HL, 1,000  $\mu\text{mol photons m}^{-2} \text{s}^{-1}$ ) or LL conditions. Light was provided with REEF-SPEC blue-white T5 lamps (Red Sea). Algal samples were flash-frozen with liquid nitrogen, freeze-dried, and stored at  $-80^\circ\text{C}$  until further analysis. Five independent samples were collected per treatment.

### Pigment Analysis

Pigment extraction, separation, and identification were performed as described in detail by Mendes et al. (2007). Briefly, approximately 4 mg of freeze-dried macroalgal samples were extracted in 1 mL of methanol-based solvent (95% methanol, 2% ammonium acetate), sonicated and incubated at  $-20^\circ\text{C}$  for 20 min in the dark. Pigment extracts were filtered through 0.2  $\mu\text{m}$  PTFE membrane filters and immediately injected into a Prominence-i LC2030C HPLC system (Shimadzu, Japan). Chromatographic separation was performed with a Supelcosil C18 column (250 mm length; 4.6 mm diameter; 5  $\mu\text{m}$  particles; Sigma-Aldrich, United States) for reverse phase chromatography and a 35 min elution program. The solvent gradient followed Kraay et al. (1992), with an injection volume of 50  $\mu\text{L}$  and a flow rate of 0.6  $\text{mL min}^{-1}$ . Pigments were identified from retention times and absorption spectra. Concentrations were calculated from the signal in the photodiode array (PDA) detector, using calibration curves constructed with pure crystalline standards (DHI group, Hørsholm, Denmark).

### Lipid Extraction

Lipids were extracted using modified Bligh and Dyer method (Bligh and Dyer, 1959; Rey et al., 2020a), where chloroform was replaced with the less hazardous dichloromethane (Cequier-Sainchez et al., 2008). Freeze-dried macroalgal biomass (50 mg) was homogenized with a mortar and pestle to obtain small flakes and then mixed with methanol (2.5 mL) and dichloromethane (1.25 mL) in a glass centrifuge tube. After vigorous homogenization and short sonication (1 min), samples were incubated on ice for 150 min on an orbital shaker (Stuart equipment, Bibby Scientific, Stone, United Kingdom). After centrifugation at 2,000 rpm for 10 min, the organic phase was transferred to another glass tube, followed by addition of water (2.25 mL) and dichloromethane (1.25 mL). Organic phase was collected after centrifugation at 2,000 rpm for 10 min. The aqueous phase was re-extracted with dichloromethane (2 mL), and organic phase was collected after centrifugation and combined with the first. Extraction was repeated on the original biomass, and the resulting organic phase was combined with the previous. Lipid extracts were dried under

a nitrogen stream and preserved at  $-20^{\circ}\text{C}$  until further analysis.

## Polar Lipidome Analysis

Polar lipidome analysis was performed according to Rey et al. (2020a). Total lipid extracts were analyzed by hydrophilic interaction liquid chromatography on a HPLC Ultimate 3000 Dionex with autosampler coupled online to a high-resolution Q-Exactive mass spectrometer (Thermo Fisher Scientific, Bremen, Germany), with a solvent system including two mobile phases (A: 25% water—50% acetonitrile—25% methanol, 5 mM ammonium acetate; B: 60% acetonitrile—40% methanol 5 mM ammonium acetate). Initially, 5% of mobile phase A was held isocratically for 2 min, followed by a linear increase to 48% of A for 8 min. A new linear increase to 65% of A for 5 min was followed by a maintenance period of 2 min, returning to the initial conditions in 3 min and held for 10 min. Analytic samples (100  $\mu\text{L}$ ) were prepared by mixing 20  $\mu\text{L}$  of lipid extract eluted in dichloromethane (lipid concentration: 2  $\mu\text{g mL}^{-1}$ ) with 8  $\mu\text{L}$  of internal standard mix (dMPC—0.04  $\mu\text{g}$ , dMPE—0.04  $\mu\text{g}$ , SM (d18:1/17:0)—0.04  $\mu\text{g}$ , 19 Lyso-PC—0.04  $\mu\text{g}$ , dPPI—0.08  $\mu\text{g}$ , CL(14:0)<sub>4</sub>—0.16  $\mu\text{g}$ , dMPG—0.024  $\mu\text{g}$ , dMPA—0.16  $\mu\text{g}$ , Cer (d18:1/17:0)—0.08  $\mu\text{g}$ , dMPS—0.08  $\mu\text{g}$ ) and 72  $\mu\text{L}$  of eluent (95% mobile phase B, 5% mobile phase A). A volume of 5  $\mu\text{L}$  of each sample was injected into Ascentis Si HPLC Pore column (10 cm  $\times$  2.1 mm, 2.7  $\mu\text{m}$ , Sigma-Aldrich), with a flow rate of 200  $\mu\text{L min}^{-1}$  at  $35^{\circ}\text{C}$ .

Acquisition of LC-MS and MS/MS data was performed in positive and negative modes (electrospray voltage 3.0 and  $-2.7$  kV, respectively), using positive/negative switching toggles, with capillary temperature of  $350^{\circ}\text{C}$  and sheath gas flow of 20 U. In MS experiments, a high resolution of 70,000, automatic gain control (AGC) target of  $1 \times 10^6$ , and maximum injection time (IT) of 100 ms were applied. For MS/MS determinations, a resolution of 17,500, AGC target of  $1 \times 10^5$  and IT of 50 ms were used. The cycles consisted in one full scan mass spectrum, and 10 data-dependent MS/MS scans that were repeated continuously throughout the experiments, with dynamic exclusion of 60 s and intensity threshold of  $2 \times 10^4$ . Normalized collision energy<sup>TM</sup> (CE) ranged between 20, 25, and 30 eV. Data acquisition was performed using the Xcalibur data system (V3.3, Thermo Fisher Scientific, United States).

Polar lipid species were identified by the  $m/z$  ratio of the ions observed in LC-MS spectra, mass accuracy of  $\leq 5$  ppm and typical retention time. Confirmation of lipid species was done by detailed analysis of MS/MS spectra. MS/MS fragmentation patterns characteristic for the polar lipid classes, including the polar head groups and fatty acyl chains, were previously described (Rey et al., 2017, 2020a,b). Ion peak integration and assignments were performed using MZmine version 2.53, based on an in-house lipid database. Previous studies on *C. tomentosum* (Rey et al., 2020a,b) were consulted as reference lipidome. Peaks with raw intensity lower than  $1 \times 10^4$  were excluded. Integrated peaks were normalized by dividing the peak areas of the extracted ion chromatograms (XIC) of each lipid species of each lipid class by the peak area of the internal standard selected for the class (Octave, Matlab).

## Statistical Analysis

Changes in the total pigment pool were assessed by principal component analysis (PCA). Variance of the content of single pigments was tested using repeated measures partly nested ANOVA. Box-plots, interaction-plots and Pearson's residuals analyses were used to verify normality and homogeneity of variance and absence of block-by/within-block interactions. Sphericity assumption was verified using Mauchly's test. Pairwise *post hoc* comparisons were performed using Welch's two-samples *t*-test. These analyses were carried out using R (R Core Team, 2018).

Lipidomic data assessment was performed using MetaboAnalyst (Xia et al., 2015). Data filtering was performed using relative standard deviation (RSD = SD/mean). Normalized data were log transformed and auto scaled. PCA were performed to visualize the general 2D clustering. Heat maps were performed using Euclidean distance measure and Ward clustering algorithm, considering the top 25 variables that most contributed to variability (PLS-DA vip). Differences in lipid content were analyzed with Welch's two-samples *t*-test (R Core Team, 2018).

## RESULTS

### Light-Induced Changes in Pigment Content

A total of nine characteristic photosynthetic pigments were identified in *C. tomentosum* and *B. plumosa*: chlorophylls *a* and *b* (Chl *a*, Chl *b*), siphonaxanthin, and its ester siphonaxanthin dodecenoate (Siph, Siph-do) as main light harvesting pigments; *t*-Neo, 9'-*cis*-neoxanthin (*c*-Neo), and Viola as typical xanthophylls; and  $\epsilon,\epsilon$ - and  $\beta,\epsilon$ -carotenes (referred hereafter as  $\epsilon$ -Car and  $\alpha$ -Car, respectively) (Table 1). The general light response was consistent in both species, with HL acclimation leading to significant changes in the composition of chlorophylls and carotenoids (Figure 1). Samples of *B. plumosa* acclimated to HL presented a drastic decline of the main light harvesting pigments (significantly different for Chl *a*, Chl *b*, Siph, and Siph-do), while the effect was less pronounced in *C. tomentosum*, with no significant change for Chl *a* content. Regarding carotenoids, both species presented highly significant accumulation of *t*-Neo and Viola under high light. Only in *B. plumosa* a decrement of pigment concentration per dried weight for *c*-Neo,  $\epsilon$ - and  $\alpha$ -Car was observed.

Principal component analysis (Figure 2) showed a clear separation between HL and LL conditions in both species, with *x*- and *y*-axis explaining, respectively 69.1 and 18.3% of variance in *C. tomentosum*, 76.5, and 11.9% in *B. plumosa*. In particular, LL samples formed a unique cluster with no difference between time points, while HL macroalgae formed separate clusters that gradually separate during 7 days of acclimation, with the samples at day 0 being the closest and day 7 the farthest from the LL cluster. ANOVA analysis (Supplementary Table 1) showed that both factors (irradiance and time) and their interaction had a significant effect on the variance of most pigment (expressed as

**TABLE 1** | Pigment composition of *Codium tomentosum* and *Bryopsis plumosa* analyzed with HPLC.

Pigment	Abbreviation	Retention time (min)	$\lambda_{max}$ (nm)
Siphonaxanthin	Siph	10.41	448
all- <i>trans</i> -Neoxanthin	<i>t</i> -Neo	11.38	418; 441; 470
9'- <i>cis</i> -Neoxanthin	<i>c</i> -Neo	12.00	413; 437; 466
Violaxanthin	Viola	13.00	416; 441; 471
Siphonaxanthin dodecenoate	Siph-do	18.53	455
Chlorophyll <i>b</i>	Chl <i>b</i>	22.63	458; 597; 645
Chlorophyll <i>a</i>	Chl <i>a</i>	24.22	430; 617; 662
$\epsilon$ -Carotene	$\epsilon$ -Car	28.14	418; 441; 471
$\alpha$ -Carotene	$\alpha$ -Car	28.33	447; 476

Pigments names, abbreviations, average retention times, and absorption maxima ( $\lambda_{max}$ ) are reported. For comparison, see Mendes et al. (2007).

pigment:Chl *a* ratios) for both species, with stronger impact on the main light harvesting pigments (Chls *a* and *b*, Siph, and Siph-do), *t*-Neo and Viola. This result was consistent between both species of macroalgae.

## Time-Dependent Accumulation of All-*Trans*-Neoxanthin and Violaxanthin

In both macroalgal species, HL had the strongest effect on the concentrations of xanthophylls *t*-Neo and Viola. As shown in **Figure 3**, these pigments were accumulated during 7 days of acclimation to HL, with a positive correlation between their concentrations and the time of exposure. In particular, Viola was accumulated in significant concentrations already after 1 day, while *t*-Neo started accumulating from day 2, and kept increasing throughout the HL acclimation period. This pattern was consistent between *C. tomentosum* and *B. plumosa*. The light- and time-dependent accumulation effect was not observed for *c*-Neo, with concentrations fluctuating around the initial level without showing a particular pattern (**Supplementary Figure 1**). Pigment to Chl *a* ratios of *c*-Neo, Siph, Siph-do, Chl *b*,  $\epsilon$ - and  $\alpha$ -Car are reported in **Supplementary Figure 1**.

Coherently with these results, in the PCA analysis (**Figure 2**), *t*-Neo and Viola resulted as the variables that most affected the trend of differentiation of HL samples within the week of acclimation (showed by the respective red arrows pointing in the direction of the HL acclimated clusters). Accordingly, as showed by ANOVA (**Supplementary Table 1**) the effect of all considered factors (irradiance, time of exposure, and their interaction) was greatest on Viola and *t*-Neo compared to other pigments ( $p$  value  $< 0.001$  for all factors and interaction) in both species.

## Polar Lipids Identification

The present study focused on the identification of lipid species belonging to the three classes of polar lipids, namely glycolipids, phospholipids, and betaine lipids, as previously reported for *C. tomentosum* (Rey et al., 2017, 2020a,b). We identified a total of 275 lipid species in *C. tomentosum* and 191 in *B. plumosa*, belonging to glycolipids (86 in *C. tomentosum*; 64 in *B. plumosa*),

phospholipids (142 in *C. tomentosum*; 120 in *B. plumosa*), and betaine lipids (47 in *C. tomentosum*; 7 in *B. plumosa*) classes.

In particular, *C. tomentosum* lipidome included: (i) for glycolipids, monogalactosyl diacylglycerols (MGDG), monogalactosyl monoacylglycerols (MGMG), digalactosyl diacylglycerols (DGDG), digalactosyl monoacylglycerols (DGMG), sulfoquinovosyl diacylglycerols (SQDG), and sulfoquinovosyl monoacylglycerols (SQMG); (ii) for phospholipids: phosphatidylcholines (PC), phosphatidylethanolamines (PE), phosphatidylglycerols (PG), and phosphatidylinositols (PI), with the respective lyso-forms (LPC, LPE, LPG, LPI); and (iii) for betaine lipids: diacylglyceryl-N,N,N trimethyl homoserines (DGTS) and monoacylglyceryl-N,N,N trimethyl homoserines (MGTS).

The same lipid classes (except for SQMG and LPI) were also present in *B. plumosa*, but with a lower number of lipid species for each lipid class. The complete list of all identified molecular species with relative quantification and fatty acyl chains is reported in **Supplementary Table 2**.

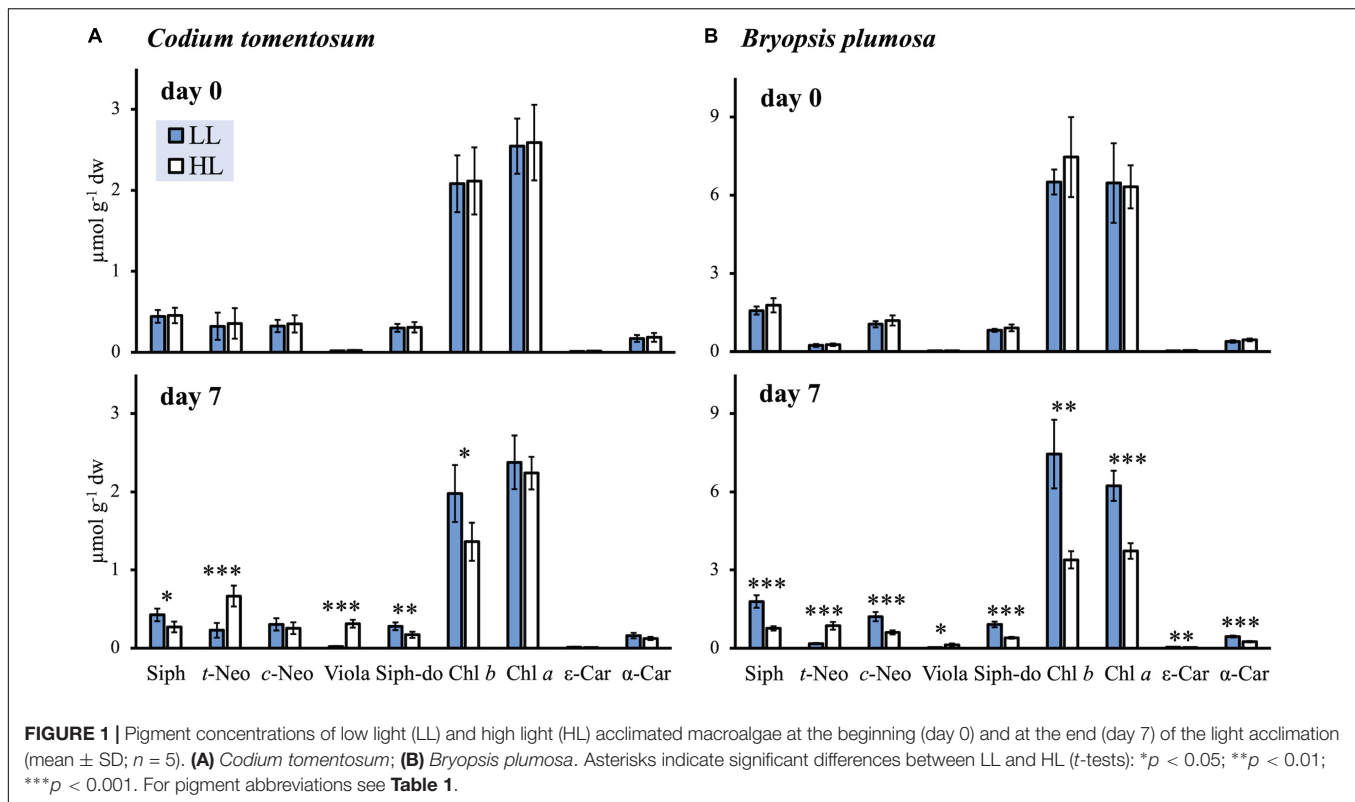
## Light-Induced Changes in the Polar Lipidome

Considering the general lipid profile of *C. tomentosum* (**Figure 4**), few quantitative changes could be observed under HL. Although most lipid classes did not present significant content alterations (normalized XIC areas), we observed a significant increment of the lyso-glycolipids MGMG (**Figure 4B**) and lyso-betaine lipids MGTS under HL (**Figure 4F**).

On the other hand, *B. plumosa* presented more pronounced quantitative changes to several lipid classes (**Figure 5**): different glycolipids, DGDG and SQDG (**Figure 5A**), and phospholipids classes, PC and PE (**Figure 5C**), increased significantly under HL, while other phospholipids decreased (i.e., PG and LPG) (**Figures 5C,D**). *B. plumosa* also presented a significant increase of some betaine lipids (i.e., DGTS) (**Figure 5E**). However, in this macroalgal species betaine lipids were generally present with extremely low concentrations in both treatments (**Figures 5E,F**). Changes under HL within relevant molecular species, analyzed with multivariate analyses (PCA and heatmap/clustering) by lipid class (i.e., glycolipids, phospholipids, and betaine lipids), are described next.

### Glycolipids

In HL acclimated *C. tomentosum*, despite a clear clustering was not observed in the PCA performed on the whole glycolipid dataset (**Figure 6A**), a trend of differentiation emerged from the heatmap/clustering analysis of the 25 glycolipid molecular species that most contributed to discriminate between treatments (**Figure 6B**). In particular, several lyso-glycolipids containing C16 fatty acyl chains [i.e., MGMG(16:3), MGMG(16:0), MGMG(16:4), and SQMG(16:0)] increased under HL. Also, other glycolipids species with similar composition of fatty acids [i.e., MGDG(34:1), DGDG(34:1), SQDG(34:1); MGDG(34:2), DGDG(34:2), and SQDG(34:2)] increased under HL in *C. tomentosum*. These glycolipid species are all characterized by the presence of C16 and C18 fatty acids in their acyl chains (**Supplementary Table 2**). Similarly, other relevant species for



the differentiation of HL samples presented a combination of fatty acids including a C16 fatty acyl chain with different number of unsaturations [MGDG(34:4) and (36:4); DGDG(34:3)] (**Supplementary Table 2**).

In *B. plumosa*, the glycolipid pool presented a more drastic response to HL, with a clear differentiation of the HL samples cluster in the PCA (**Figure 6C**) and a decrease of all 25 most relevant molecular species (mostly represented by MGDG) in the heatmap/clustering analysis (**Figure 6D**). The trend of MGDG species observed was opposite to the quantitative increase of other glycolipid classes (DGDG and SQDG) previously reported under HL (**Figure 5A**).

Notably some of the identified species that most contributed to variability (PLS-DA vip) [i.e., MGDG(36:4), MGDG(38:5), DGDG(36:2), and DGDG(38:5)] displayed the same decreasing trend in both *C. tomentosum* and *B. plumosa* (**Figures 6B,D**).

### Phospholipids

Principal component analysis, performed with the complete molecular species dataset of phospholipids, did not show a separation of HL acclimated *C. tomentosum* (**Figure 7A**). Nonetheless, heatmap/clustering analysis performed on the 25 molecular species that most contributed to differentiation, showed a clear separation of HL samples after 7 days of acclimation (**Figure 7B**). The phospholipids involved belonged mostly to PG and PC classes. In particular, it was observed an increase of molecular species with polyunsaturated fatty acids, often presenting 18:3 or 18:4 fatty acyl chains [LPC(18:4); PC(30:4), PC(32:4), PC(32:6), PC(32:7), PC(34:3), PC(34:4), PC(34:7), PC(36:6), PC(36:7), PC(38:8), PC(38:9);

PI(34:4); PG(34:4), PG(40:3), PG(40:4), PG(40:6), and PG(42:4)] (**Figure 7B** and **Supplementary Table 2**).

A similar trend was observed in *B. plumosa* (**Figures 7C,D**). In this case, together with PC and PG a relevant contribution of different PE species was observed. Increasing phospholipid species with polyunsaturated fatty acids were also reported [PC(34:4), PC(34:3), PC(34:6), PC(36:7), PC(44:4); PE(34:3), PE(34:4), PE(34:6), PE(36:4), PE(36:5), PE(36:7), and PE(38:6)], characterized by the presence of C18 or longer polyunsaturated fatty acyl chains (**Figure 7D** and **Supplementary Table 2**).

Similarly to the glycolipids analysis, some of the highlighted phospholipid species had a consistent trend in both *C. tomentosum* and *B. plumosa* [i.e., PC(32:3), PC(32:4), PC(34:3), PC(34:4), and PC(36:7)] (**Figures 7B,D**).

### Betaine Lipids

In *C. tomentosum*, while PCA of the complete betaine lipids dataset did not show evident separation of HL cluster (**Figure 8A**) (as for glycolipids and phospholipids), heatmap/clustering analysis showed a general trend of increase of all 25 molecular species that most contribute to differentiation after 7 days of HL acclimation (**Figure 8B**). This analysis showed not only the increase of several lyso-betaine lipids (MGTS), coherently with previous observations (**Figure 4F**), but also of different DGTS species. Several of these key betaine lipid species were esterified to polyunsaturated fatty acids, frequently with C18 or longer chains [MGTS(16:3), MGTS(16:4), MGTS(18:3), MGTS(18:4), MGTS(20:4), MGTS(20:5), MGTS(22:6), and MGTS(22:5); DGTS(32:3), DGTS(32:4), DGTS(34:3), DGTS(34:4), DGTS(34:6), DGTS(36:6), DGTS(36:3), DGTS(36:7),

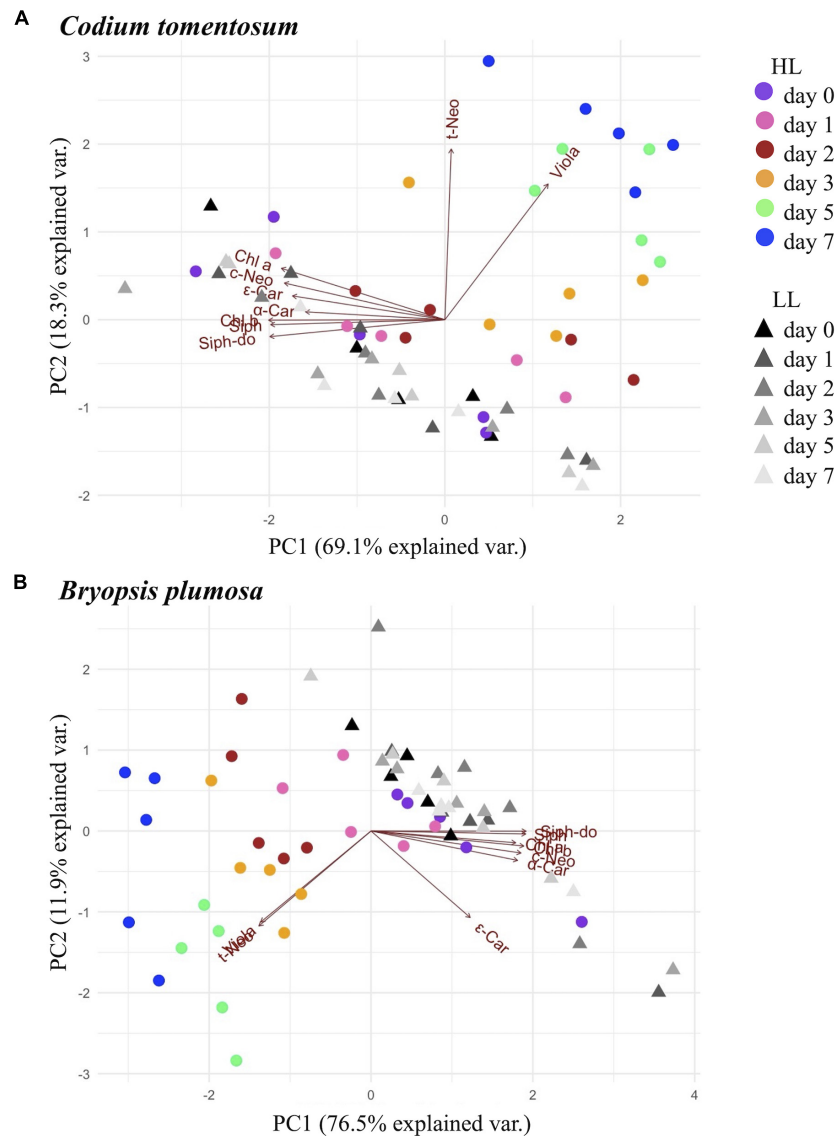


**FIGURE 2** | Principal component analysis (PCA) analysis of pigments ( $\mu\text{mol g}^{-1}$  dw) in Bryopsidales macroalgae during 7 days of low and high light acclimation. **(A)** *Codium tomentosum*; **(B)** *Bryopsis plumosa*.

DGTS(34:7), DGTS(42:10), and DGTS(42:11)] (**Figure 8B** and **Supplementary Table 2**). A similar trend was previously reported in phospholipids (**Figure 7B** and **Supplementary Table 2**).

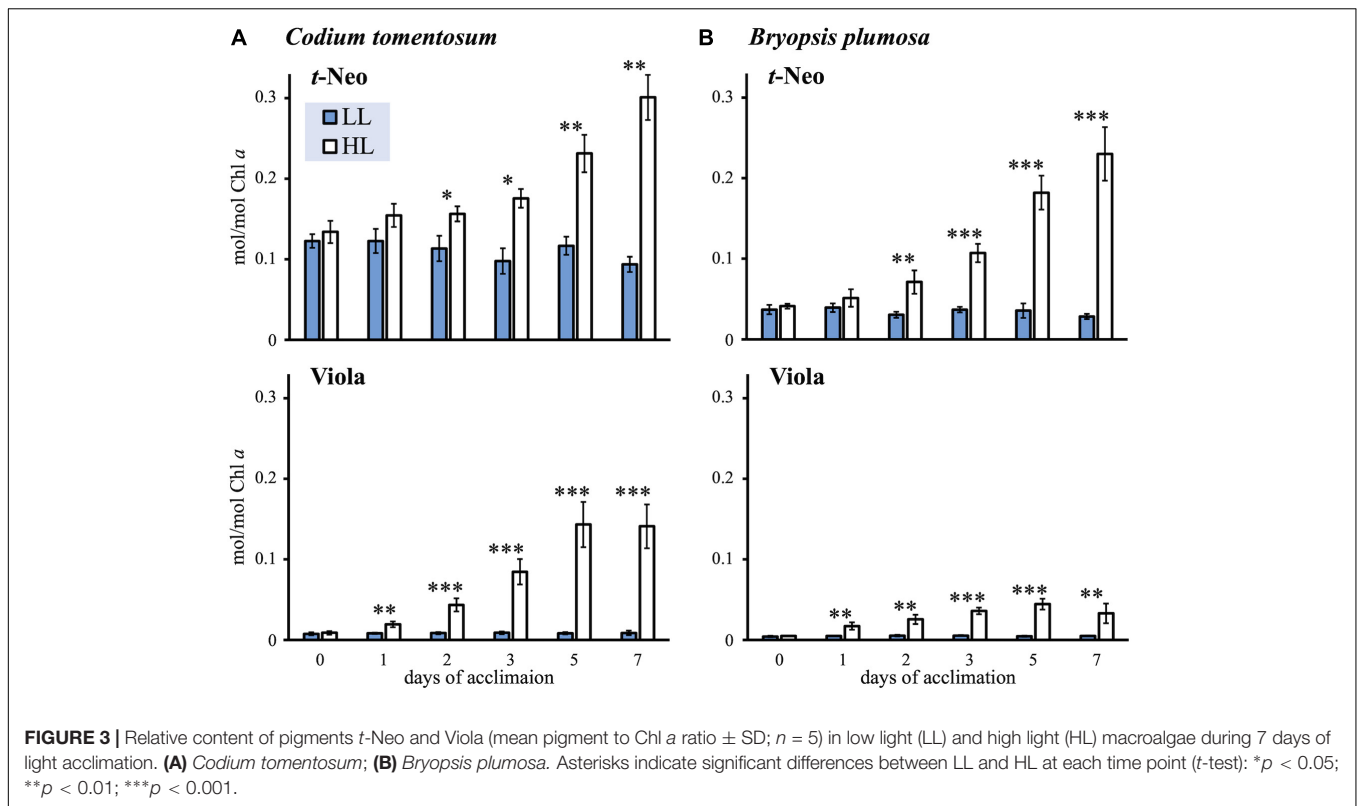
Given that only seven molecular species of betaine lipids were identified in *B. plumosa*, with considerably low concentrations (**Figures 5E,F** and **Supplementary Table 2**), the relative data was excluded from this analysis.

## DISCUSSION

### Pigment Contribution to Excess Energy Regulation

*Codium tomentosum* and *B. plumosa* presented the expected pigment pool for Bryopsidales algae (Yokohama et al., 1977;

Nakayama and Okada, 1990; Cruz et al., 2015). In both species, acclimation to higher irradiance determined: (i) a general decrease of light harvesting pigments (namely Chls *a* and *b*, Siph, Siph-do), a known high light acclimation response in plants and algae and (ii) a change in the xanthophyll composition, involving a time-dependent accumulation of *t*-Neo and Viola. These results are coherent with previously reported studies performed on different species of Bryopsidales (Uragami et al., 2014; Cartaxana et al., 2018) and demonstrate a trend of acclimation to higher irradiances. Furthermore, the detailed characterization of the time-dependent changes in the pigment composition of both *C. tomentosum* and *B. plumosa* indicate that the response to high light can be faster (within one to two days of high light exposure) than previously reported (1–2 weeks) under lower irradiances (Uragami et al., 2014; Cartaxana et al., 2018).



The accumulation of *t*-Neo and Viola under high light has been previously correlated with the oligomerization of siphonaxanthin–chlorophyll–protein complexes (SCP) of photosystem II (PSII) in *Codium intricatum*, leading to the hypothesis that these pigments might contribute to the dissipation of excessive light energy (Uragami et al., 2014). Indeed, according to this model the oligomerization of SCP would determine a decrease of energy transfer to PSII, by adjusting the distance between energy donor (SCP) and acceptor (PSII core). A precedent study also reported a correlation between oligomerization of antenna complexes (isolated from *Bryopsis corticulans*) and the dissociation of Chl *b*, reducing the light absorption capabilities of SCP (Chen et al., 2005). Therefore, this process could also represent an additional sink of excitation energy in the *t*-Neo-mediated oligomerization of SCP proposed by Uragami et al. (2014). In most algae and plant taxa—with the only exception of the ancient green alga lineages of Mesostigmatophyceae (Yoshii et al., 2003) and Bryopsidales (Qin et al., 2015)—the *cis* isomer of neoxanthin (*c*-Neo) represents the sole molecular form associated with antenna complexes, while *t*-Neo is not associated with light harvesting or photoprotection (Takaichi and Mimuro, 1998). Hence, the involvement of *t*-Neo in photoprotection could represent a unique mechanism of Bryopsidales (Giossi et al., 2020). The presence of such photoprotective activity could represent a safety valve for the dissipation of excess excitation energy under higher irradiances, particularly relevant for these algae that lack a functional xanthophyll cycle (Franklin et al., 1996; Raniello et al., 2004, 2006; Cruz et al., 2015; Christa et al., 2017; Giovagnetti et al., 2018),

an important and ubiquitous photoprotection mechanism in aquatic and terrestrial oxygenic phototrophs (Latowski et al., 2011; Goss and Lepetit, 2015).

Our results also show the co-occurrent accumulation of *t*-Neo and Viola, with a relevant pattern. During one week of acclimation to HL, Viola is already accumulated at day 1, while *t*-Neo begins to be significantly accumulated only at day 2 (Figure 3). The accumulation of both these pigments clearly contributed to the differentiation of samples during HL acclimation, as showed in PCA analysis (Figure 2). Viola is known as the biochemical precursor of *t*-Neo, within the  $\beta$ -branch of carotenoid biosynthetic pathway (Lohr, 2011), and this biochemical relationship explains the contextual accumulation of these pigments. It has also been proposed that Viola could participate in the energy tuning at the level of SCP together with *t*-Neo, given that both xanthophylls present the same weak interactions with the SCP (Uragami et al., 2014), possibly allowing fast and reversible interactions with the antenna complexes. Therefore, despite the role of Viola in the theorized photoprotective model remains unclear, the present work shows that this pigment is clearly involved in this photoacclimation process and is essential for the accumulation of *t*-Neo. During HL acclimation we also observed a putative accumulation of other carotenoids belonging to the same  $\beta$ -branch of carotenoid biosynthesis (namely antheraxanthin, zeaxanthin, and  $\beta$ -carotene), but the relative HPLC signal was too close to the detection limit to ensure their correct identification and quantification (data not shown). We propose that the synthesis of these carotenoids might also increase under higher irradiances

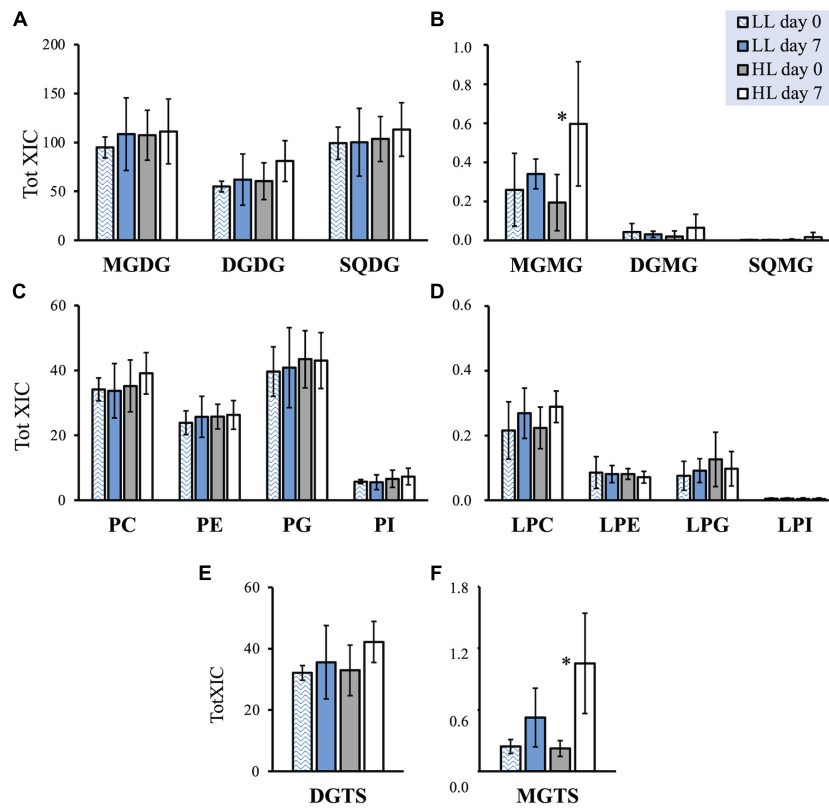


**FIGURE 4** | Sum of the normalized extracted ion chromatograms (XIC) areas (mean  $\pm$  SD;  $n = 5$ ) of the peaks identified for the lipids species of glycolipid, phospholipid, and betaine lipid classes in *Codium tomentosum* exposed to low light (LL) and high light (HL), at the beginning (day 0) and at the end (day 7) of the light acclimation. **(A)** Glycolipids (MGDG, DGDG, SQDG); **(B)** Lyso-forms of glycolipids (MGMG, DGMG, SQMG); **(C)** Phospholipids (PC, PE, PG, PI); **(D)** Lyso-forms of phospholipids (LPC, LPE, LPG, LPI); **(E)** Betaine lipids (DGTS); **(F)** Lyso-forms of betaine lipids (MGTS). Asterisks indicate significant differences between day 0 and day 7, within the same light condition ( $t$ -test):  $*p < 0.05$ .

or longer acclimation than that used in this study, due to their role as biochemical precursors of Viola and  $t$ -Neo in the pathway of carotenoid biosynthesis (Lohr, 2011).

## Patterns of Lipid Differentiation Under High Light

While the lipidome characterization obtained for *C. tomentosum* was consistent with previous studies (Da Costa et al., 2015; Rey et al., 2017, 2020a,b), we found no available literature information on the lipidome of *B. plumosa*. The number of lipid species identified was higher in *C. tomentosum* (275 lipid species) than in *B. plumosa* (191 lipid species). High light acclimation caused more significant changes in the lipidome of *B. plumosa* than that of *C. tomentosum* (Figures 4–7), which could be linked to the greater complexity of the polar lipidome of *C. tomentosum* (i.e., higher number of identified lipid species) determining higher plasticity during acclimation. Most likely, in the presence of such rich and plastic polar lipidome, the imposed HL treatment (1,000  $\mu\text{mol photons m}^{-2} \text{s}^{-1}$  for 1 week) was not sufficient for triggering a more drastic response in this species. Also, our target Bryopsidales are characterized by completely different macromorphologies: *C. tomentosum* displays a thick thallus,

divided in an external photosynthetic region that hosts the chloroplasts and an internal colorless region (called medulla), while *B. plumosa* is formed by several thin filaments, all originating from a central segment and forming different layers (Graham and Wilcox, 2000; Lee, 2008). All these features possibly make the observed light acclimation response species-specific: the polar lipidome of wild specimens of *C. tomentosum* (like those collected and cultured for our study) could be more efficient in responding to environmental changes compared to cultured strains of *B. plumosa*. Nonetheless, heatmap/clustering analyses allowed to highlight several meaningful trends in both target species.

Under HL conditions, *C. tomentosum* accumulated some phospholipid species (i.e., PG and PC) and betaine lipids presenting fatty acyl chains with higher level of unsaturation (Figures 7, 8). The presence of polyunsaturated fatty acids could be linked with a photoprotective role within the thylakoid membranes, since they could contribute to the scavenging of reactive oxygen species (ROS; Mène-Saffrané et al., 2009; Schmid-Siegert et al., 2016). A similar trend of polyunsaturated fatty acid increase was observed in *B. plumosa*'s glycolipids and phospholipids (Figures 6, 7). Additionally, in *C. tomentosum* we reported an increase of lyso-forms of glycolipids (MGMG)

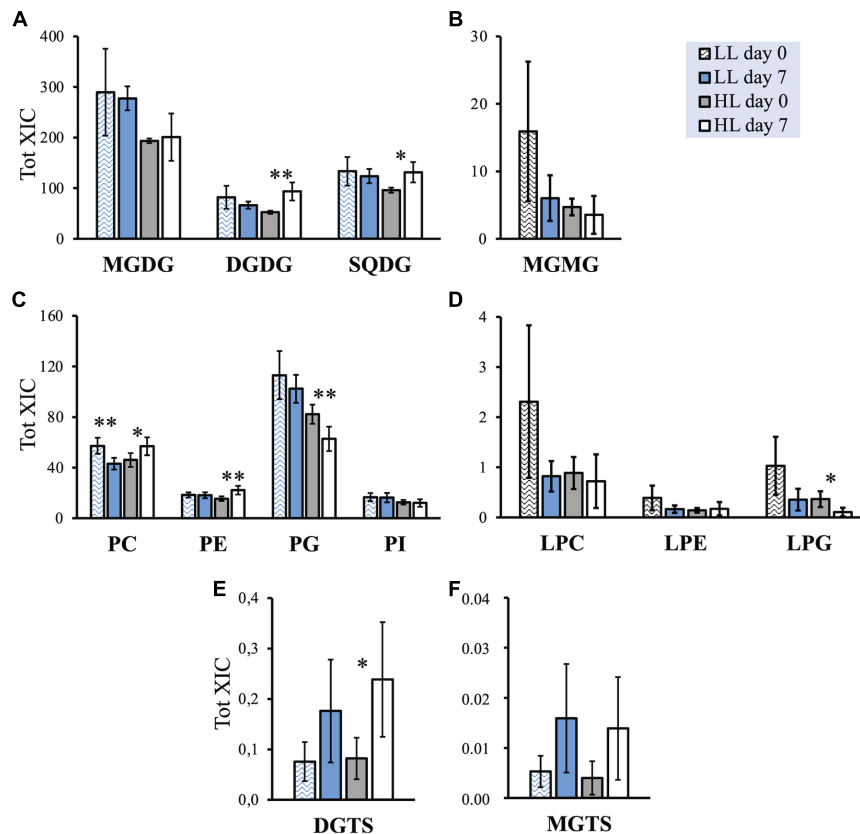


**FIGURE 5** | Sum of the normalized extracted ion chromatograms (XIC) areas (mean  $\pm$  SD;  $n = 5$ ) of the peaks identified for the lipids species of glycolipid, phospholipid, and betaine lipid classes in *Bryopsis plumosa* exposed to low light (LL) and high light (HL), at the beginning (day 0) and at the end (day 7) of the light acclimation. **(A)** Glycolipids (MGDG, DGDG, SQDG); **(B)** Lyso-forms of glycolipids (MGMG, DGMG); **(C)** Phospholipids (PC, PE, PG, PI); **(D)** Lyso-forms of phospholipids (LPC, LPG); **(E)** Betaine lipids (DGTS); **(F)** Lyso-forms of betaine lipids (MGTS). Lipid species with values close or equal to 0 (DGMG, SQMG, and LPI) are not reported. Asterisks indicate significant differences between day 0 and day 7, within the same light condition ( $t$ -test): \* $p < 0.05$ ; \*\* $p < 0.01$ .

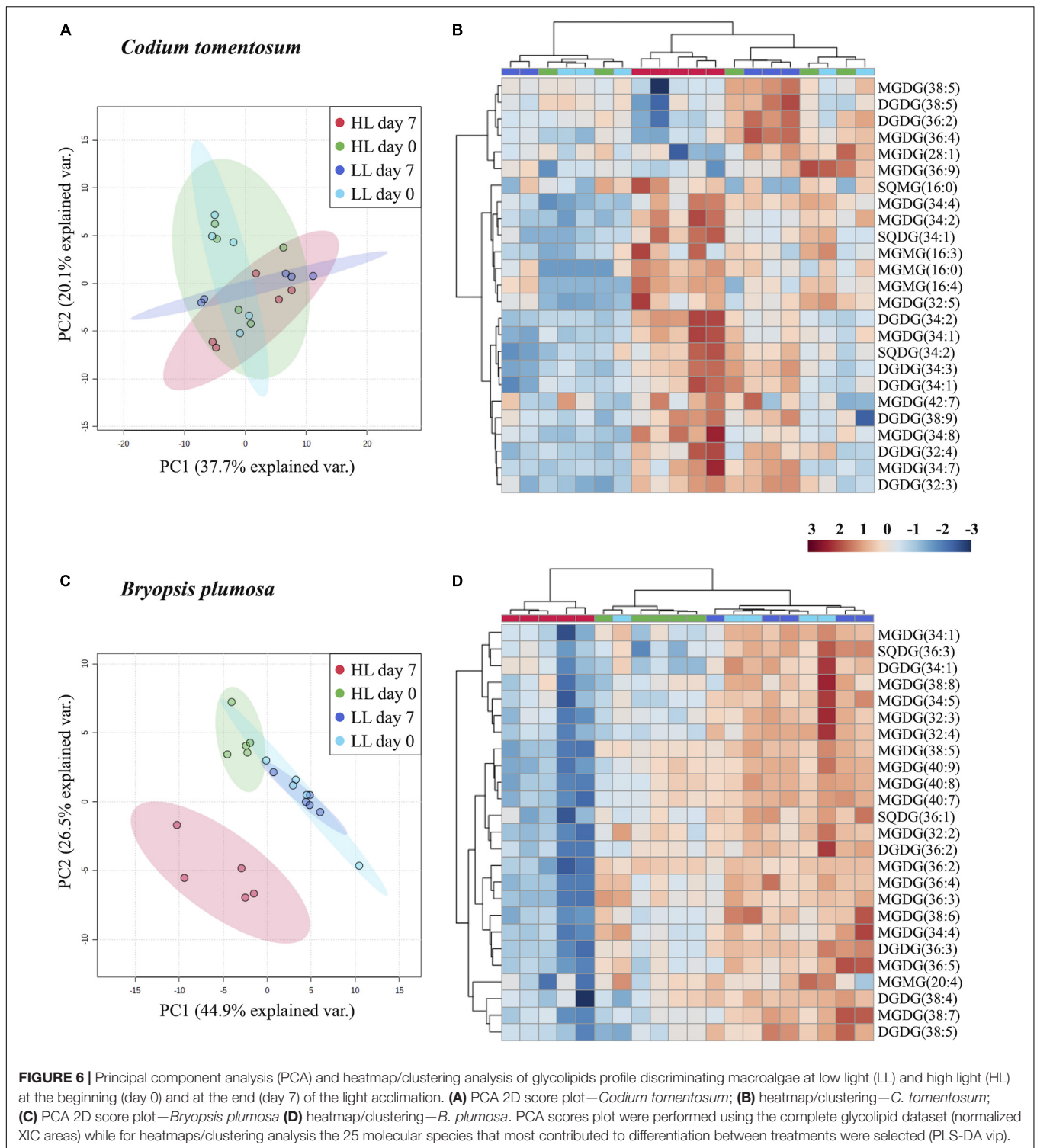
(Figures 4, 6). Cleavage of MGDG into MGMG could be related to their role in ROS scavenging (Schmid-Siebert et al., 2016). A similar trend was observed for lyso-betaine lipids: MGTS increased under HL (Figures 4, 8), indicating that acclimation to higher irradiance could lead to cleavage of a fatty acyl chain. In the case of MGMG, we observed a trend of increase of C16 fatty acids. It is known that these fatty acyl chains are esterified in the sn-2 position of glycolipids in the plastid membranes of green algae (Li-Beisson et al., 2015). For this reason, the increase of C16 lyso-glycolipids may represent a tendency of cleavage of fatty acids in sn-1 position under HL.

Monogalactosyl diacylglycerols, DGDG, SQDG, PG, and DGTS are known to be important components of chloroplast membranes in green algae (Hölzl and Dörmann, 2007; Kobayashi et al., 2016; Jüppner et al., 2017; Li-Beisson et al., 2019). In particular, MGDG, DGDG, SQDG, and PG are considered “the essential glycerolipid quartet” in all photosynthetic eukaryotes, given that their presence is thought to be critical for maintaining an optimal photosynthetic yield (Boudière et al., 2014). Alterations in the content of the lipid species from these classes allow us to conclude that high light seemed to stimulate a remodeling of chloroplast membranes, possibly allowing a

better response to increased irradiance. Finally, despite some species-specific differences, common differentiation trends could be identified in both *C. tomentosum* and *B. plumosa*, leading to the conclusion that high-light acclimation response of the polar lipidome presents some shared patterns between different Bryopsidales species.

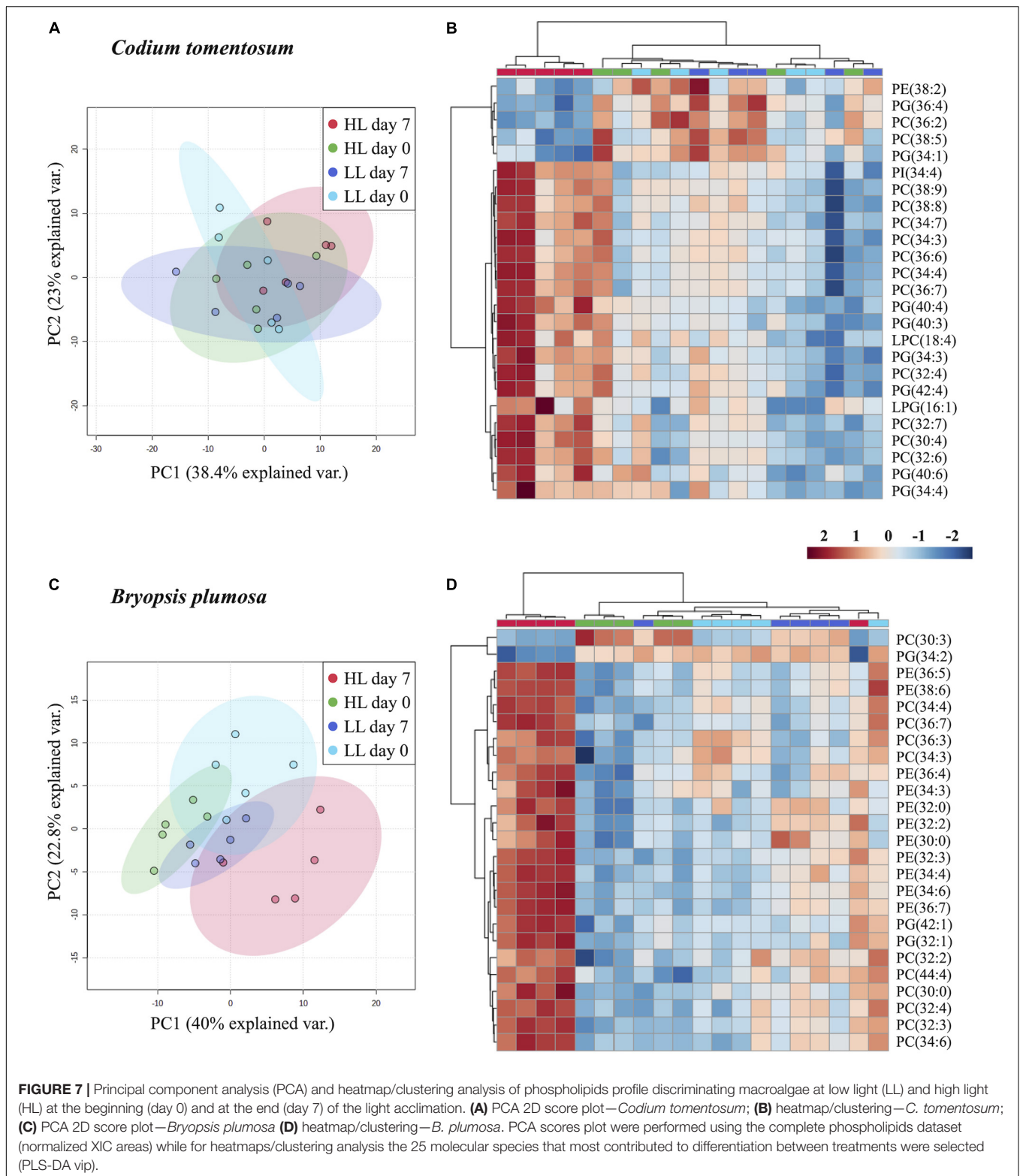
## Pigment-Lipid Interactions Within the Thylakoid Membranes

As recently reviewed (Goss and Latowski, 2020), lipids are thought to be essential for xanthophyll-mediated photoprotection, in particular in relation with the xanthophyll cycle. In diatoms and higher plants, an increase of MGDG was correlated with high solubilization of hydrophobic xanthophyll cycle pigments and of their respective rate of de-epoxidation, therefore contributing to photoprotection (Latowski et al., 2004; Goss et al., 2005). MGDG are considered essential for the re-organization of the membrane environment in which antenna complexes are immersed, allowing the interaction between xanthophyll cycle pigments and enzymes, thus contributing to the



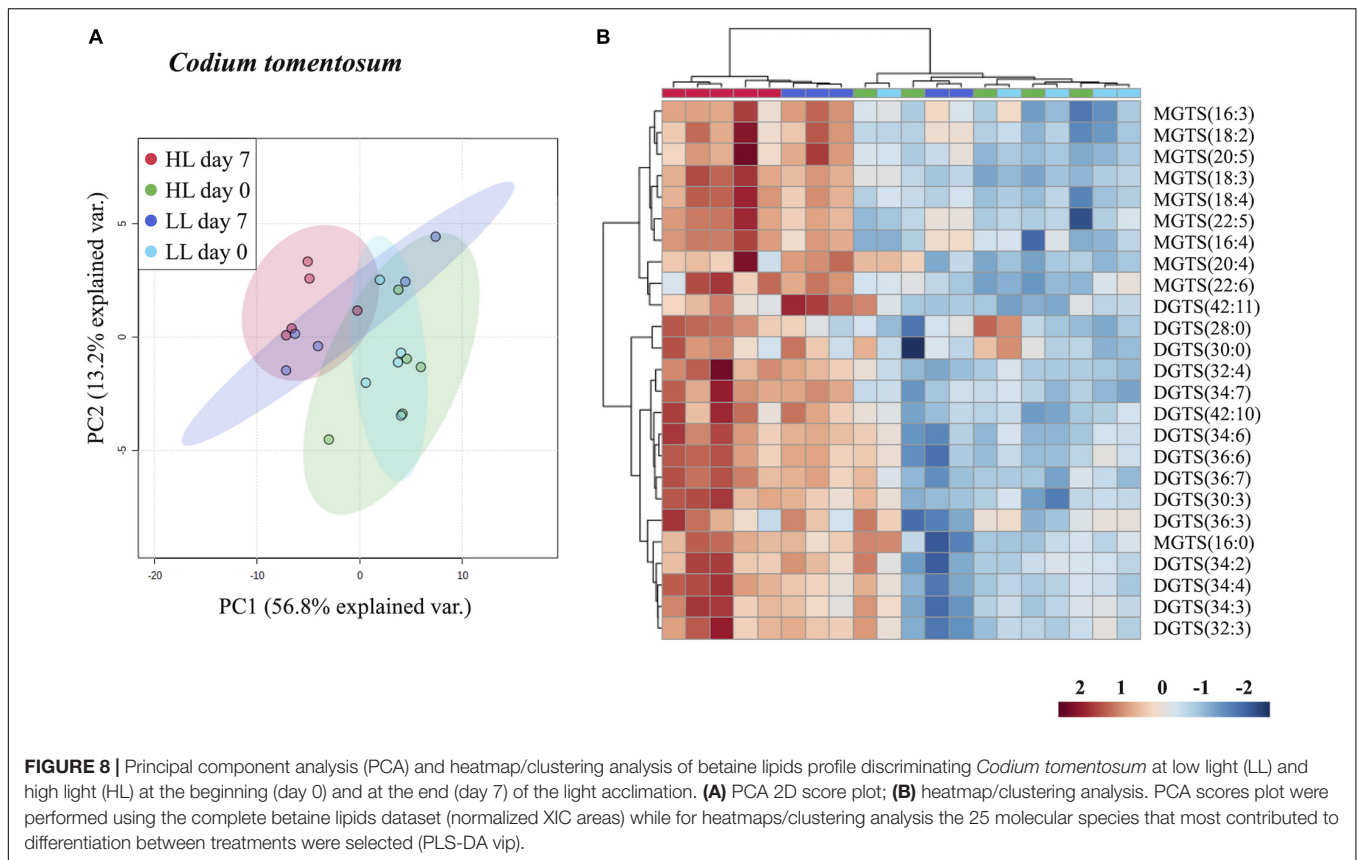
formation of the energy-dissipative quenching (Goss and Latowski, 2020). In this model, xanthophyll cycle pigments can be found either in association with the antenna complexes or immersed in the MGDG shield located around the complexes (Lepetit et al., 2010; Schaller et al., 2010).

Despite Bryopsidales were reported to lack a functional xanthophyll cycle (e.g., Christa et al., 2017), similarities can be found between the proposed model of *t*-Neo mediated oligomerization of SCP and the formation of quenching sites within functionally detached antennae oligomers of diatoms and higher plants (Miloslavina et al., 2008;



Holzwarth et al., 2009; Giossi et al., 2020). For these reasons, the rearrangement of the MGDG pool observed in our study could reflect significant changes happening in the thylakoid membrane environment of Bryopsidales,

possibly influencing the interaction between pigment and proteins within the SCP. We hypothesize that alterations of the biochemical properties of the lipid bilayer could promote the interaction between the excess of *t*-Neo



and Viola molecules, likely dissolved in the thylakoid membrane, with SCP.

Contextually, the reported trend of increase in relevant membrane lipids with higher number of unsaturations could also contribute to increase the fluidity of the membrane environment, possibly allowing faster interaction of *t*-Neo and Viola with the SCP and contributing to the instauration of a rapid and reversible oligomerization and separation of the complexes. It is possible that all of these processes would contribute to the proposed *t*-Neo-mediated photoprotective model (Uragami et al., 2014).

## CONCLUSION

Due to scarce data on the general photophysiology of Bryopsidales, the function of high light-dependent accumulation of *t*-Neo and Viola in this group of algae remains to be elucidated. Nonetheless, we clearly show the co-occurrence of increased levels of these pigments with a shift in the polar lipidome composition that could reflect a rearrangement of the thylakoid membranes under high light, possibly contributing to the onset of the theorized neoxanthin-mediated photoprotection at the level of the light harvesting complexes. Observed changes in pigment and lipid composition could reduce damages to the photosynthetic apparatus under increased irradiance, thus contributing to the overall fitness of Bryopsidales algae.

## DATA AVAILABILITY STATEMENT

The original contributions presented in the study are included in the article/**Supplementary Material**, further inquiries can be directed to the corresponding author.

## AUTHOR CONTRIBUTIONS

CG, SC, and PC: conceptualization. CG, SC, RM, and PC: methodology—algae collection, cultivation, and experimental setup. PC: methodology—pigment analysis. FR, TM, and MRD: methodology—lipidomics. CG, FR, and PC: data analysis. CG: investigation and first manuscript draft. SC, FR, MRD, and PC: supervision. PC: project administration and funding acquisition. All authors contributed to manuscript revision, read, and approved the submitted version.

## FUNDING

This study received financial support from R&D project CtLight (PTDC/BIA-FBT/30979/2017) funded by European Regional Development Fund (ERDF), through COMPETE2020—Programa Operacional Competitividade e Internacionalização (POCI), and by national funds (OE), through Fundação para a Ciência e a Tecnologia—Ministério da Ciência, Tecnologia e Ensino

Superior (FCT/MCTES). FCT/MCTES also provided financial support to CESAM (UIDP/50017/2020+UIDB/50017/2020), LAQV-REQUIMTE (UIDB/50006/2020), and RNEM (LISBOA-01-0145-FEDER-402-022125). Equipment was funded by PORBIOTA project (POCI-01-0145-FEDER-022127) through POCI and Programa Operacional Regional de Lisboa, ERDF, and by FCT/MCTES through national funds (PIDAC).

## ACKNOWLEDGMENTS

FR (CEECIND/00580/2017), SC (2020.03278.CEECIND), and PC (CEECIND/01434/2018) acknowledge individual funding by FCT/MCTES in the scope of the Individual Call to Scientific Employment Stimulus. TM acknowledges individual funding by project Omics4Algae (POCI-01-0145-FEDER-030962). The authors also thank Diana Lopes for technical assistance. The

## REFERENCES

- Andersen, R. A. (2005). *Algal Culturing Techniques*. Burlington: Elsevier Academic Press.
- Anderson, J. M. (1983). Chlorophyll-protein complexes of a *Codium* species, including a light-harvesting siphonaxanthin-Chlorophyll *a/b*-protein complex, an evolutionary relic of some Chlorophyta. *Biochim. Biophys. Acta Bioenerg.* 724, 370–380. doi: 10.1016/0005-2728(83)90096-8
- Arata, P. X., Quintana, I., Canelón, D. J., Vera, B. E., Compagnone, R. S., and Ciancia, M. (2015). Chemical structure and anticoagulant activity of highly pyruvylated sulfated galactans from tropical green seaweeds of the order Bryopsidales. *Carbohydr. Polym.* 122, 376–386. doi: 10.1016/j.carbpol.2014.10.030
- Bligh, E. G., and Dyer, W. J. (1959). A rapid method of total lipid extraction and purification. *Can. J. Biochem. Physiol.* 37, 911–917. doi: 10.1139/c59-099
- Boudière, L., Michaud, M., Petroustos, D., Rébeillé, F., Falconet, D., Bastien, O., et al. (2014). Glycerolipids in photosynthesis: composition, synthesis and trafficking. *Biochim. Biophys. Acta Bioenerg.* 1837, 470–480. doi: 10.1016/j.bbabi.2013.09.007
- Cartaxana, P., Morelli, L., Quintaneiro, C., Calado, G., Calado, R., and Cruz, S. (2018). Kleptoplast photoacclimation state modulates the photobehaviour of the solar-powered sea slug *Elysia viridis*. *J. Exp. Biol.* 221:jeb180463. doi: 10.1242/jeb.180463
- Cequier-Sainchez, E., Rodriíguez, C., Ravelo, A. G., and Zairate, R. (2008). Dichloromethane as a solvent for lipid extraction and assessment of lipid classes and fatty acids from samples of different natures. *J. Agric. Food Chem.* 56, 4297–4303. doi: 10.1021/jf073471e
- Chen, H., Shen, S., Liang, Y., Leng, J., Tang, M., and Gong, Y. (2005). Evidence for dissociation of chlorophyll *b* from the main light-harvesting complex in the oligomerization state isolated from marine alga, *Bryopsis corticulans*. *Biochim. Biophys. Acta Bioenerg.* 1707, 170–178. doi: 10.1016/j.bbabi.2004.12.001
- Christa, G., Cruz, S., Jahns, P., de Vries, J., Cartaxana, P., Esteves, A. C., et al. (2017). Photoprotection in a monophyletic branch of chlorophyte algae is independent of energy-dependent quenching (qE). *New Phytol.* 214, 1132–1144. doi: 10.1111/nph.14435
- Cremon, M. C. M., Leliart, F., West, J., Lam, D. W., Shimada, S., Lopez-Bautista, J. M., et al. (2019). Reassessment of the classification of Bryopsidales (Chlorophyta) based on chloroplast phylogenomic analyses. *Mol. Phylogenet. Evol.* 130, 397–405. doi: 10.1016/j.ympev.2018.09.009
- Cruz, S., Cartaxana, P., Newcomer, R., Dionísio, G., Calado, R., Seródio, J., et al. (2015). Photoprotection in sequestered plastids of sea slugs and respective algal sources. *Sci. Rep.* 5:7904. doi: 10.1038/srep07904
- Da Costa, E., Melo, T., Moreira, A. S. P., Alves, E., Domingues, P., Calado, R., et al. (2015). Decoding bioactive polar lipid profile of the macroalgae *Codium tomentosum* from a sustainable IMTA system using a lipidomic approach. *Algal Res.* 12, 388–397. doi: 10.1016/j.algal.2015.09.020
- authors acknowledge that part of the data presented in this manuscript was generated in the aim of a master's thesis (Giossi, 2020).
- ## SUPPLEMENTARY MATERIAL
- The Supplementary Material for this article can be found online at: <https://www.frontiersin.org/articles/10.3389/fmars.2021.745083/full#supplementary-material>
- Supplementary Figure 1** | Content of *c*-Neo, Siph, Siph-do, Chl *b*,  $\epsilon$ - and  $\alpha$ -Car (pigment:Chl *a* ratios, mean  $\pm$  SD; *n* = 5) of low light (LL) and high light (HL) grown macroalgae during 7 days of light acclimation. **(A)** *Codium tomentosum*; **(B)** *Bryopsis plumosa*. Asterisks indicate significant differences between LL and HL at each time point (*t*-test): \**p* < 0.05; \*\**p* < 0.01; \*\*\**p* < 0.001. *c*-Neo: 9'-*cis*-Neoxanthin, Siph: Siphonaxanthin, Siph-do: Siphonaxanthin dodecenoate, Chl *b*: Chlorophyll *b*,  $\epsilon$ -Car:  $\epsilon$ -Carotene; and  $\alpha$ -Car:  $\alpha$ -Carotene.
- Fleurence, J., and Levine, I. (2016). *Seaweed in Health and Disease Prevention*. London: Elsevier Academic Press.
- Franklin, L. A., Seaton, G. G. R., Lovelock, C. E., and Larkum, A. W. D. (1996). Photoinhibition of photosynthesis on a coral reef. *Plant Cell Environ.* 19, 825–836. doi: 10.1111/j.1365-3040.1996.tb00419.x
- Giossi, C. (2020). *Photoacclimation and Photoprotection Strategies in Siphonous Green Algae of the Order Bryopsidales (Codium tomentosum and Bryopsis plumosa)*. Master's thesis. Ravenna: University of Bologna.
- Giossi, C., Cartaxana, P., and Cruz, S. (2020). Photoprotective role of neoxanthin in plants and algae. *Molecules* 25:4617. doi: 10.3390/molecules25204617
- Giovagnetti, V., Han, G., Ware, M. A., Ungerer, P., Qin, X., Wang, W.-D., et al. (2018). A siphonous morphology affects light-harvesting modulation in the intertidal green macroalga *Bryopsis corticulans* (Ulvophyceae). *Planta* 247, 1293–1306. doi: 10.1007/s00425-018-2854-5
- Goss, R., and Latowski, D. (2020). Lipid dependence of xanthophyll cycling in higher plants and algae. *Front. Plant Sci.* 11:455. doi: 10.3389/fpls.2020.00455
- Goss, R., and Lepetit, B. (2015). Biodiversity of NPQ. *J. Plant Physiol.* 172, 13–32. doi: 10.1016/j.jplph.2014.03.004
- Goss, R., Lohr, M., Latowski, D., Grzyb, J., Vieler, A., Wilhelm, C., et al. (2005). The role of hexagonal structure forming lipids in diadinoxanthin and violaxanthin solubilization and de-epoxidation. *Biochemistry* 44, 4028–4036. doi: 10.1021/bi047464k
- Graham, L. E., and Wilcox, L. W. (2000). *Algae*. Upper Saddle River, NJ: Prentice-Hall.
- Hözl, G., and Dörmann, P. (2007). Structure and function of glycolipids in plants and bacteria. *Prog. Lipid Res.* 46, 225–243. doi: 10.1016/j.plipres.2007.05.001
- Holzwarth, A. R., Miloslavina, Y., Nilkens, M., and Jahns, P. (2009). Identification of two quenching sites active in the regulation of photosynthetic light-harvesting studied by time-resolved fluorescence. *Chem. Phys. Lett.* 483, 262–267. doi: 10.1016/j.cplett.2009.10.085
- Jüppner, J., Mubeen, U., Leisse, A., Caldana, C., Brust, H., Steup, M., et al. (2017). Dynamics of lipids and metabolites during the cell cycle of *Chlamydomonas reinhardtii*. *Plant J.* 92, 331–343. doi: 10.1111/tpj.13642
- Kageyama, A., Yokohama, Y., Shimura, S., and Ikawa, T. (1977). An efficient excitation energy transfer from a carotenoid, siphonaxanthin to chlorophyll *a* observed in a deep-water species of chlorophyte seaweed. *Plant Cell Physiol.* 18, 477–480. doi: 10.1093/oxfordjournals.pcp.a075458
- Kobayashi, K., Endo, K., and Wada, H. (2016). "Roles of Lipids in Photosynthesis," in *Lipids in Plant and Algae Development*, eds Y. Nakamura and Y. Li-Beisson (Cham: Springer International Publishing), 21–49. doi: 10.1007/978-3-319-25979-6\_2
- Kraay, G. W., Zapata, M., and Veldhuis, M. J. W. (1992). Separation of chlorophylls *c1*, *c2*, and *c3* of marine phytoplankton by reversed-phase C18 high-performance liquid chromatography. *J. Phycol.* 28, 708–712. doi: 10.1111/j.0022-3646.1992.00708.x

- Latowski, D., Åkerlund, H. E., and Strzałka, K. (2004). Violaxanthin de-epoxidase, the xanthophyll cycle enzyme, requires lipid inverted hexagonal structures for its activity. *Biochemistry* 43, 4417–4420. doi: 10.1021/bi049652g
- Latowski, D., Kuczyńska, P., and Strzałka, K. (2011). Xanthophyll cycle—a mechanism protecting plants against oxidative stress. *Redox Rep.* 16, 78–90. doi: 10.1179/174329211X13020951739938
- Lee, R. E. (2008). *Phycology*. Cambridge: Cambridge University Press.
- Lepetit, B., Volke, D., Gilbert, M., Wilhelm, C., and Goss, R. (2010). Evidence for the existence of one antenna-associated, lipid-dissolved and two protein-bound pools of diadinoxanthin cycle pigments in diatoms. *Plant Physiol.* 154, 1905–1920. doi: 10.1104/pp.110.166454
- Li-Beisson, Y., Beisson, F., and Riekhof, W. (2015). Metabolism of acyl-lipids in *Chlamydomonas reinhardtii*. *Plant J.* 82, 504–522. doi: 10.1111/tpj.12787
- Li-Beisson, Y., Thelen, J. J., Fedosejevs, E., and Harwood, J. L. (2019). The lipid biochemistry of eukaryotic algae. *Prog. Lipid Res.* 74, 31–68. doi: 10.1016/j.plipres.2019.01.003
- Lohr, M. (2011). “Carotenoid metabolism in phytoplankton,” in *Phytoplankton Pigments -Characterization, Chemotaxonomy and Applications in Oceanography*, eds S. Roy, C. Llewellyn, E. S. Egeland, and G. Johnsen (Cambridge: Cambridge University Press), 113–162. doi: 10.1017/CBO9780511732263.006
- Maeda, R., Ida, T., Ihara, H., and Sakamoto, T. (2012). Immunostimulatory activity of polysaccharides isolated from *Caulerpa lentillifera* on macrophage cells. *Biosci. Biotechnol. Biochem.* 76, 501–505. doi: 10.1271/bbb.110813
- Mendes, C. R., Cartaxana, P., and Brotas, V. (2007). HPLC determination of phytoplankton and microphytobenthos pigments: comparing resolution and sensitivity of a C18 and a C8 method. *Limnol. Oceanogr. Methods* 5, 363–370. doi: 10.4319/lom.2007.5.363
- Méne-Saffrané, L., Dubugnon, L., Chételat, A., Stolz, S., Gouhier-Darimont, C., and Farmer, E. E. (2009). Nonenzymatic oxidation of trienoic fatty acids contributes to reactive oxygen species management in *Arabidopsis*. *J. Biol. Chem.* 284, 1702–1708. doi: 10.1074/jbc.M807114200
- Miloslavina, Y., Wehner, A., Lambrev, P. H., Wientjes, E., Reus, M., Garab, G., et al. (2008). Far-red fluorescence: a direct spectroscopic marker for LHCII oligomer formation in non-photochemical quenching. *FEBS Lett.* 582, 3625–3631. doi: 10.1016/j.febslet.2008.09.044
- Nakayama, K., and Okada, M. (1990). Purification and characterization of light-harvesting chlorophyll *a/b*-protein complexes of photosystem II from the green alga, *Bryopsis maxima*. *Plant Cell Physiol.* 31, 253–260. doi: 10.1093/oxfordjournals.pcp.a077900
- Paul, N. A., Neveux, N., Magnusson, M., and de Nys, R. (2014). Comparative production and nutritional value of “sea grapes”—the tropical green seaweeds *Caulerpa lentillifera* and *C. racemosa*. *J. Appl. Phycol.* 26, 1833–1844. doi: 10.1007/s10811-013-0227-9
- Pérez-Lloréns, J., Hernández, I., Brun, F., Vergara, J., and León, Á. (2018). *Those Curious and Delicious Seaweeds. A Fascinating Voyage from Biology to Gastronomy*. Cadiz: Editorial UCA.
- Qin, X., Wang, W., Chang, L., Chen, J., Wang, P., Zhang, J., et al. (2015). Isolation and characterization of a PSI–LHCI super-complex and its sub-complexes from a siphonaceous marine green alga, *Bryopsis Corticulans*. *Photosynth. Res.* 123, 61–76. doi: 10.1007/s11120-014-0039-z
- R Core Team (2018). *R: A language and Environment for Statistical Computing*. Vienna: R Foundation for Statistical Computing.
- Raniello, R., Lorenti, M., Brunet, C., and Buia, M. (2004). Photosynthetic plasticity of an invasive variety of *Caulerpa racemosa* in a coastal Mediterranean area: light harvesting capacity and seasonal acclimation. *Mar. Ecol. Prog. Ser.* 271, 113–120. doi: 10.3354/meps271113
- Raniello, R., Lorenti, M., Brunet, C., and Buia, M. C. (2006). Photoacclimation of the invasive alga *Caulerpa racemosa* var. *cylindracea* to depth and daylight patterns and a putative new role for siphonaxanthin. *Mar. Ecol.* 27, 20–30. doi: 10.1111/j.1439-0485.2006.00080.x
- Rey, F., Cartaxana, P., Melo, T., Calado, R., Pereira, R., Abreu, H., et al. (2020a). Domesticated populations of *Codium tomentosum* display lipid extracts with lower seasonal shifts than conspecifics from the wild— relevance for biotechnological applications of this green seaweed. *Mar. Drugs* 18, 188. doi: 10.3390/md18040188
- Rey, F., Da Costa, E., Campos, A. M., Cartaxana, P., MacIel, E., Domingues, P., et al. (2017). Kleptoplasty does not promote major shifts in the lipidome of macroalgal chloroplasts sequestered by the sacoglossan sea slug *Elysia viridis*. *Sci. Rep.* 7, 1–10. doi: 10.1038/s41598-017-12008-z
- Rey, F., Melo, T., Cartaxana, P., Calado, R., Domingues, P., Cruz, S., et al. (2020b). Coping with starvation: contrasting lipidomic dynamics in the cells of two sacoglossan sea slugs incorporating stolen plastids from the same macroalgae. *Integr. Comp. Biol.* 60, 43–56. doi: 10.1093/icb/icaa019
- Santos, S. A. O., Vilela, C., Freire, C. S. R., Abreu, M. H., Rocha, S. M., and Silvestre, A. J. D. (2015). Chlorophyta and Rhodophyta macroalgae: a source of health promoting phytochemicals. *Food Chem.* 183, 122–128. doi: 10.1016/j.foodchem.2015.03.006
- Schaller, S., Latowski, D., Jemioła-Rzemińska, M., Wilhelm, C., Strzałka, K., and Goss, R. (2010). The main thylakoid membrane lipid monogalactosyldiacylglycerol (MGDG) promotes the de-epoxidation of violaxanthin associated with the light-harvesting complex of photosystem II (LHCII). *Biochim. Biophys. Acta Bioenerg.* 1797, 414–424. doi: 10.1016/j.bbabi.2009.12.011
- Schmid-Siegert, E., Stepushenko, O., Glauser, G., and Farmer, E. E. (2016). Membranes as structural antioxidants recycling of malondialdehyde to its source in oxidation-sensitive chloroplast fatty acids. *J. Biol. Chem.* 291, 13005–13013. doi: 10.1074/jbc.M116.729921
- Takaichi, S., and Mimuro, M. (1998). Distribution and geometric isomerism of neoxanthin in oxygenic phototrophs: 9'-cis, a sole molecular form. *Plant Cell Physiol.* 39, 968–977. doi: 10.1093/oxfordjournals.pcp.a029461
- Uragami, C., Galzerano, D., Gall, A., Shigematsu, Y., Meisterhans, M., Oka, N., et al. (2014). Light-dependent conformational change of neoxanthin in a siphonous green alga, *Codium intricatum*, revealed by Raman spectroscopy. *Photosynth. Res.* 121, 69–77. doi: 10.1007/s11120-014-0011-y
- Wang, W., Qin, X., Sang, M., Chen, D., Wang, K., Lin, R., et al. (2013). Spectral and functional studies on siphonaxanthin-type light-harvesting complex of photosystem II from *Bryopsis corticulans*. *Photosynth. Res.* 117, 267–279. doi: 10.1007/s11120-013-9808-3
- Xia, J., Sinelnikov, I. V., Han, B., and Wishart, D. S. (2015). MetaboAnalyst 3.0—making metabolomics more meaningful. *Nucleic Acids Res.* 43, W251–W257. doi: 10.1093/nar/gkv380
- Yokohama, Y., Kageyama, A., Ikawa, T., and Shimura, S. (1977). A carotenoid characteristic of Chlorophycean seaweeds living in deep coastal waters. *Bot. Mar.* 20, 433. doi: 10.1515/botm.1977.20.7.433
- Yoshii, Y., Takaichi, S., Maoka, T., and Inouye, I. (2003). Photosynthetic pigment composition in the primitive green alga *Mesostigma viride* (Prasinophyceae): phylogenetic and evolutionary implications. *J. Phycol.* 39, 570–576. doi: 10.1046/j.1529-8817.2003.02098.x

**Conflict of Interest:** The authors declare that the research was conducted in the absence of any commercial or financial relationships that could be construed as a potential conflict of interest.

**Publisher's Note:** All claims expressed in this article are solely those of the authors and do not necessarily represent those of their affiliated organizations, or those of the publisher, the editors and the reviewers. Any product that may be evaluated in this article, or claim that may be made by its manufacturer, is not guaranteed or endorsed by the publisher.

Copyright © 2021 Giossi, Cruz, Rey, Marques, Melo, Domingues and Cartaxana. This is an open-access article distributed under the terms of the Creative Commons Attribution License (CC BY). The use, distribution or reproduction in other forums is permitted, provided the original author(s) and the copyright owner(s) are credited and that the original publication in this journal is cited, in accordance with accepted academic practice. No use, distribution or reproduction is permitted which does not comply with these terms.